Scientific Visualization, 2024, volume 16, number 3, pages 48 - 59, DOI: 10.26583/sv.16.3.05

On Visualization When Controlling Wave Structures Using Distributed Heat Sources

A.K. Alekseev[1,B], A.E. Bondarev[2,A]

[A] Keldysh Institute of Applied Mathematics RAS
[B] RSC Energia, Korolev, Russia

[1] ORCID: 0000-0001-8317-8688, aleksey.k.alekseev@gmail.com
[2] ORCID: 0000-0003-3681-5212, bond@keldysh.ru

Abstract

For two-dimensional Euler equations, flow control using spatially distributed stationary heat sources is considered. The initial flow, characterized by the interaction of Edney - type shock waves, was changed with the help of heat sources in such a way as to reduce the maximum pressure on the surface of the body. The problem was solved in an optimization formulation using conjugate equations to calculate the gradient of the target functional. In addition to visualizing flow parameters in this problem, it is of interest to visualize the distribution of adjoint parameters and heat sources.

Keywords: Euler equations, interaction of shock waves, heat sources, flow structure control, adjoint equations.

Introduction

Active control of the flow using various methods of influence, including the release of energy in the flow field [1-7], is an urgent problem, which is still quite far from a satisfactory solution. One of the areas of application is the control of flows in which the interaction of shocks of *IV* the Edney classification is realized [8,9]. When oblique and direct shock waves intersect, there are six different types of interaction [8], which differ greatly both in the flow structure and in the values of pressure and heat flows on the surface of the body. Moreover, the most intense effect on the surface of the body is realized during an interaction *IV* of the Edney type . With this type of flow, a narrow stream is formed, which is decelerated in several successive oblique shock waves and reaches the surface of the body with small losses of total pressure. This leads to very high values of pressure and heat flow at the surface of the body. In this regard, it is of practical interest to be able to actively control the flow in order to destroy the flow structure of a type *IV* and replace it with a structure that is less dangerous, from the point of view of loads. In [3, 4], the destruction of this flow structure using pulsed heating was experimentally studied. In [5], numerical experiments demonstrated the possibility of reducing the maximum pressure and heat fluxes on the surface of a body by releasing thermal energy in the vicinity of the incident shock. Calculations have demonstrated the possibility of reducing the maximum pressure and heat flows on the surface of the body, however, the work indicates that the control action is not optimal in magnitude. One of the main reasons preventing the practical application of flow control methods is their fairly high energy intensity, so the question of finding the minimum impact in terms of integral value is of significant interest. Another obstacle is the high complexity of searching for zones and magnitudes of influence, so efficient computational algorithms for searching for control actions are also of interest.

In this paper, within the framework of a two-dimensional model of an inviscid gas, a method and results of searching for spatially distributed stationary heat sources of minimum

total power that reduce the maximum value of pressure on the surface of the body are presented. The main tool used is an iterative solution of the inverse problem of minimizing a certain functional using gradient methods. The gradient of the functional with respect to the sources was calculated using adjoint equations.

1. Statement of the problem.

Let us consider the flow of a supersonic flow around a flat body with a cylindrical bluntness when an inclined shock wave falls on it. We use non-stationary Euler equations:

$$\frac{\partial \rho}{\partial t} + \frac{\partial(\rho U_k)}{\partial x^k} = 0; \tag{1}$$

$$\frac{\partial\left(\rho U_i\right)}{\partial t} + \frac{\partial\left(\rho U_k U_i + P\delta_{ik}\right)}{\partial x^k} = 0; \tag{2}$$

$$\frac{\partial(\rho E)}{\partial t} + \frac{\partial(\rho U_k h_0)}{\partial x^k} + q(x,y) = 0; \tag{3}$$

here $E = \left(e + \frac{1}{2}(U^2 + V^2) \right)$, $P = (\gamma - 1)\rho e$, $\gamma = \frac{C_p}{C_v}$, $e = \frac{RT}{\gamma - 1}$, $h = \frac{\gamma}{\gamma - 1}\frac{P}{\rho} = \gamma e$.

The calculation area is rectangular $\Omega = (0 < x < X_{\max}, 0 < y < Y_{\max})$. The time interval $(0 < t < t_f)$ was selected from the conditions for establishing a stationary regime. A spatially homogeneous field was taken as the initial conditions.

At the inlet boundary we accept inflow conditions corresponding to an inclined shock wave in a homogeneous flow. We set outflow conditions at the output boundary and the lateral boundaries of the region. No-flow conditions are specified at the body boundary Γ.

Euler's equations were solved using second-order reconstruction [11], methods [12] and [13] for solving the Riemann problem, and the fourth-order method [14]. For the second-order method, it was possible to reproduce a *IV* type circuit on a grid 200×200, for a 4th-order accurate circuit on a grid 100×100. Boundary conditions on the body are implemented by the immersed boundary method [15-17].

Figure 1 shows density isolines for a type IV configuration , corresponding to the operating conditions [5] and obtained in calculations on a grid 400×475 using [11,13] . Flow parameters: $M = 6$, flow deflection angle behind the shock $\Theta_1 = 15^o$, $\gamma = 1.4$. Figure 2 shows the pressure distribution in the flow field in three-dimensional form.

As the oblique shock moved upward along the coordinate, Y a sequential transition from a *III* type scheme through a *IV* type scheme to a *V* type scheme was observed. In this case, the flow according to the scheme *IV* has varieties that differ significantly in pressure on the body [19]. At low pressures Y (at the border with the circuit *III*) the pressure is maximum, then, as it increases Y , a second maximum is observed; finally, the circuit *IV* turns into a circuit *IVa* in which the high-pressure jet bends upward and does not hit the body, which leads to a decrease in the maximum pressure.

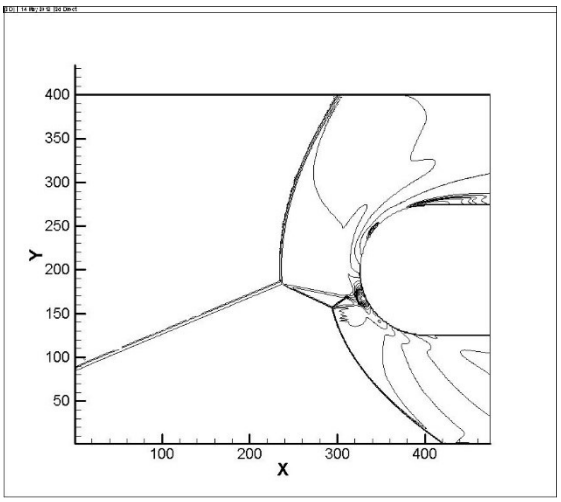

Figure 1. Density isolines for IV the type of interaction

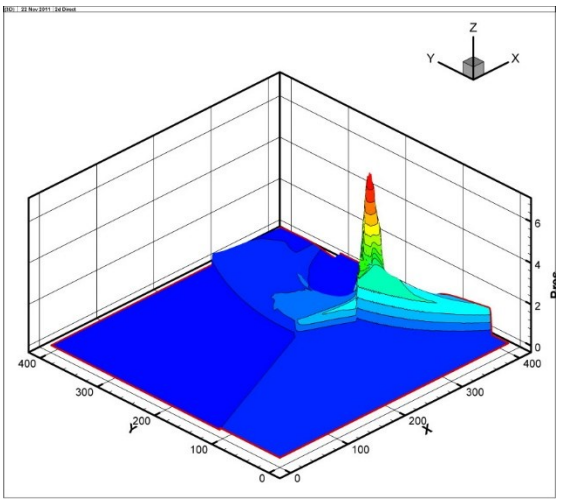

Figure 2. Pressure distribution for IV the type of interaction

There are several possible scenarios for the transition from a type IV configuration to more favorable structures. In [5], due to the heat source, the shock wave is deflected, leading to a transformation of the IV type flow pattern to the V type pattern. In [1], a complete restructuring of the flow with the formation of a forward separation zone ("thermal needle") is considered. Both of these options involve the use of a localized point source. Here we will consider a spatially distributed field of thermal sources.

2. Optimal control problem

Let us consider a steady flow with an interaction IV of the type, Fig. 1.2. We need to select a heat flow distribution $q(x,y)$ that changes the flow pattern so as to minimize the maximum static pressure on the surface of the body:

$$\varepsilon(q) = \max_{\Gamma} p = \int_{\Gamma} p\delta(s - s_{\max})d\Gamma\,, \tag{4}$$

($s_{\max}$ - coordinates of the point of maximum pressure on the body) . At the same time, the integral power of thermal sources

$$\eta = \int_{\Omega} q d\Omega \tag{5}$$

(taking into account the positivity of sources, corresponding to the norm $\|q\|_{L_1(\Omega)}$) should be minimal. Unlike works [5-7], in this work the control is carried out not with the help of an ini-

tial temperature disturbance, simulating a pulsed heat release, but with the help of time-constant heat sources.

The work also used functionals like:

$$\varepsilon(q) = 1/2\int_{\Gamma} p^n d\Gamma + \alpha/2\int_{\Omega}\left(q(x,y)\right)^2 d\Omega,\ n = 1,2,... \tag{6}$$

Increasing the indicator n in the expression $\int_{\Gamma} p^n d\Gamma$, makes the functionality more sensitive to changes in pressure and, generally speaking, allows you to more accurately identify zones of maximum pressure, which is due to the fact that $\max_{\Gamma} p = \|p\|_{L_\infty} = \lim_{n\to\infty}\left(\int_{\Gamma} p^n\right)^{1/n}$.

In expression (6), the zero-order Tikhonov regularization is used to ensure the search for the minimum disturbance. The regularization coefficient α is selected during calculations.

To calculate the gradient of the target functional, conjugate equations of the form [6,10] were used.

$$\frac{\partial\Psi_\rho}{\partial t} + \frac{\partial\Psi_i}{\partial t}U^i + \frac{\partial\Psi_e}{\partial t}E + U^k\frac{\partial\Psi_\rho}{\partial X^k} + U^kU^i\frac{\partial\Psi_i}{\partial X^k} + (\gamma-1)\frac{\partial\Psi_k}{\partial X^k}e + U^k h_0\frac{\partial\Psi_e}{\partial X^k} = 0 \tag{7}$$

$$\frac{\partial\Psi_i}{\partial t}\rho + \frac{\partial\Psi_e}{\partial t}\rho U^i + U^i\frac{\partial\Psi_k}{\partial X^i} + U^i\frac{\partial\Psi_i}{\partial X^k} + \frac{\partial\Psi_\rho}{\partial X^k} + h_0\frac{\partial\Psi_e}{\partial X^k} + U^iU^k\frac{\partial\Psi_e}{\partial X^i} = 0 \tag{8}$$

$$\frac{\partial\Psi_e}{\partial t} + \gamma U^k\frac{\partial\Psi_e}{\partial X^k} + (\gamma-1)\frac{\partial\Psi_k}{\partial X^k} = 0 \tag{9}$$

$$\text{initial conditions } \Psi_{\rho,U,V,e}\Big|_{\tau=0} = 0; \tag{10}$$

Boundary conditions (at the boundary of the computational domain): $\Psi_{\rho,U,V,e}\Big|_{\partial\Omega} = 0$.

The boundary conditions (on the body) for functional (4) have the form

$$\Psi_\rho\Big|_\Gamma = (\gamma-1)e\delta(s-s_{\max}),\ \Psi_e\Big|_\Gamma = (\gamma-1)\rho\delta(s-s_{\max}) \tag{11}$$

The boundary conditions (on the body) for functional (6) have the form

$$\Psi_\rho\Big|_\Gamma = nP^{n-1}(\gamma-1)e,\ \Psi_e\Big|_\Gamma = nP^{n-1}(\gamma-1)\rho \tag{12}$$

The form of the functional (4) leads to boundary conditions (11) containing δ – the function on the boundary. In the case of movement of the zone of maximum pressure along the surface of the body, this shape can lead to sharp changes in the associated parameters and the corresponding gradient and complicate the use of gradient methods **.** Therefore, the main part of the calculations was carried out using form (6) and boundary conditions (12). The conjugate equations were solved using the numerical method in [18] similarly to [6,7,20] . Using the results of solving the conjugate equations, one can obtain the radient of the target functional of the following form:

$$\nabla\varepsilon_q = \Psi_e(t,x,y) + \alpha q(x,y) \tag{13}$$

The search for optimal control is carried out by an iterative method using the steepest descent method

$$q^{n+1}(x,y) = q^n(x,y) - \tau\nabla\varepsilon_q \tag{14}$$

4. Calculation results for minimizing pressure on the surface

The results of gradient calculations for $\varepsilon(q) = \max_{\Gamma} p = \int_{\Gamma} p\delta(s - s_{\max})d\Gamma$ and for $\varepsilon(q) = 1/2\int_{\Gamma} p^n d\Gamma$ and $n = 1$ are $n = 2$ practically the same in shape (up to scale), which makes them equivalent when using gradient optimization methods. This is probably due to the presence of a sharp pressure maximum for this task and will not be fulfilled for tasks with a weakly expressed maximum.

The distribution of the gradient value (13) in the calculated field is presented in Figure 3 in three-dimensional form.

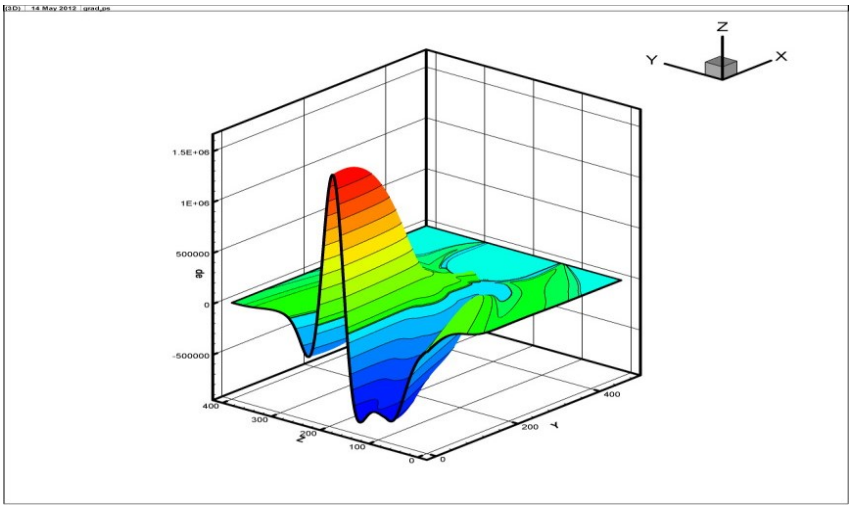

Figure 3. Gradient of the target functional in IV the interaction mode

It is possible to distinguish three zones in which heating will reduce the pressure on the surface and one which will increase the pressure. One of the zones of maximum gradient coincides with the incident shock, which corresponds to the mechanism of weakening the impact due to the deflection of the incident wave. The second corresponds to the entry of the streamline strictly into the region of the high-pressure jet, the third (minimal) corresponds to the entry of a disturbance of the opposite family relative to the falling shock. From Fig. 3 it can be seen that the gradient in different zones has different signs, which during iterations can lead to a negative density of heat sources, which is physically not realizable. In these calculations, the density of heat sources was projected in the positive direction. Each iteration corresponds to solving one direct and one conjugate problem.

The regularizing coefficient plays a special role here α. At a small value of the regularization coefficient, α heat sources completely distort the flow field. At $\alpha = 0.001$ power of thermal sources $\eta = 0.84$ (which is significantly more than in [5]) and $P_{\max} = 0.82$. The results were obtained in 9 iterations. The flow field has undergone significant restructuring; the corresponding field of heat sources and pressure are presented in Fig. 4, 5.

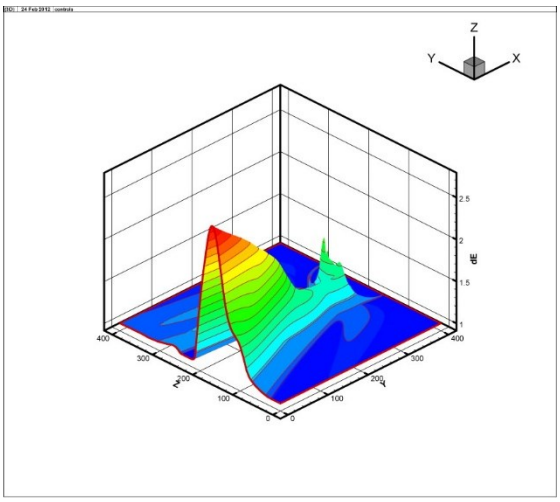

Figure 4. Heat source density $\alpha = 0.001$, $\eta = 0.84$

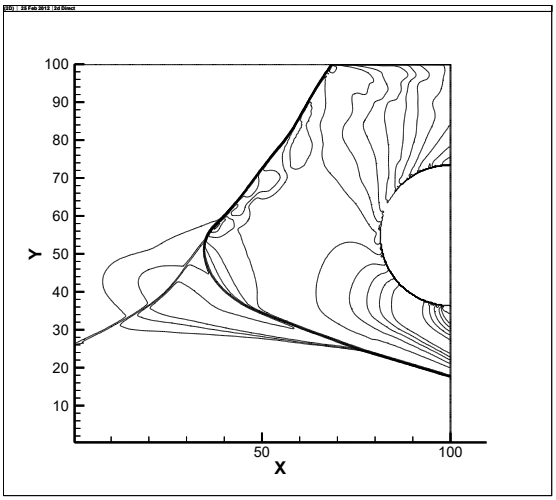

Figure 5. Isolines of the pressure field $\alpha = 0.001$, $P_{\max} = 0.82$

Increasing the regularization coefficient makes it possible to reduce the integral intensity of the sources by reducing the control efficiency (increasing the maximum pressure); the corresponding results for $\alpha = 1$, ($\eta = 0.0247$, $P_{\max} = 2.3$) are presented in Fig. 6, 7.

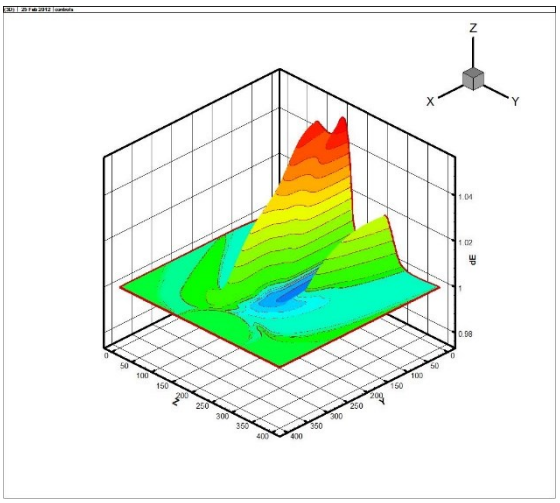

Figure 6. Heat source density, $\alpha = 1$, $\eta = 0.0247$

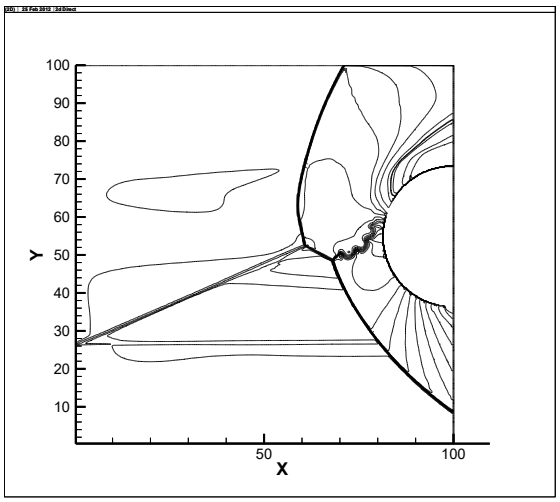

Figure 7. Isolines of the pressure field, ($\alpha = 1$), $P_{\max} = 2.3$

The results were obtained in 4 iterations. It should be noted that the flow field has undergone a restructuring corresponding to the transition to the type of interaction *IVa* [19].

Calculations demonstrate the possibility of effectively searching for control actions and the significant influence of regularization. The results of solving the inverse problem demonstrate the transformation of the flow not according to the "shock refraction" scenario with the transition from structure *IV* to *V* [5] , but the transition from interaction *IV* of type to structure of type *IVa* . In the work of Kogan and Starodubtsev [5], a heat source of the following form was used:

$$q = q_s \exp(-\frac{r^2}{r_s^2}),\ q_s = 2,\ r_s = 0.1 \qquad (15)$$

For flow parameters $M = 6$, $\Theta_1 = 15^o$ (flow deflection angle), the results of [5] are generally reproduced, and it is possible to reduce the maximum pressure value from $P_{\max} = 6.587$ to $P_{\min} = 0.88$. The required power of heat sources $\eta = 0.068$.

As another option for controlling the flow field, the "thermal needle" mode is implemented [1]. The "thermal needle" mode is presented in Fig. 8 using pressure field isolines. At the same $P_{\min} = 0.79$ time $\eta = 0.32$.

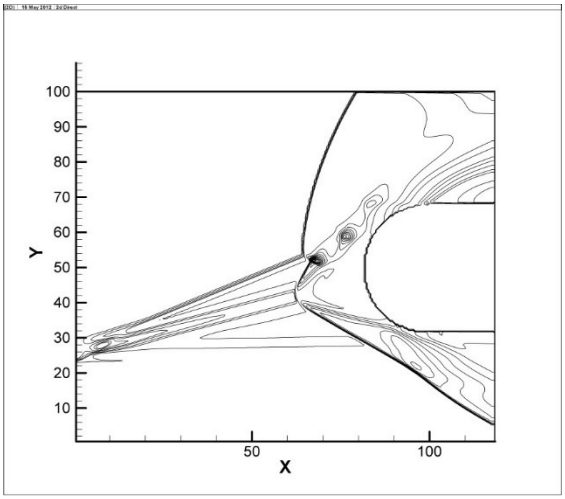

Figure 8. Isolines of the pressure field during separated flow induced by a "thermal needle"

5. Reproduction of a predetermined flow structure

The search for the distribution of heat flows that optimally reduces the pressure on the body strongly depends on the regularization coefficient and leads to different flow structures.

The transition of the flow from a structure *IV* to *V* a "thermal needle" [1] requires a radical restructuring of the flow, which comes down to a significant change in the effective shape of the streamlined body,

The flow transition from the structure *IV* to *V* the shock using local refraction [5] is also quite energy-consuming even if the heat release zone successfully hits the shock wave.

In this regard, the management of the transition from the interaction *IV* of the type purposefully to the structure of the type *IVa* described in [19] is considered. This type of structure *IVa* is characterized by the fact that the high-pressure jet bends along the body and does not fall on it.

In this regard, in this work we used the following target functional:

$$\varepsilon(q) = 1/2 \sum_{i=1}^{4} \int_{\Omega_{obs}} (f_i - f_i^{IVa})^2 dV + \alpha/2 \int_{\Omega} \left(q(x,y) \right)^2 d\Omega \qquad (16)$$

here is Ω_{obs} a region in the calculation field containing some part of the flow structure *IVa* interactions, f_i^{IVa} - flow parameters corresponding to the structure *IVa*. These parameters are taken from calculations for *IVa* type of shock interaction obtained by moving a falling shock. Thus, we purposefully strive to reproduce the known and convenient flow structure in a certain area Ω_{obs}.

Calculation results for the following functional are presented

$$\varepsilon(q) = 1/2 \int_{\Omega_{obs}} (\rho - \rho^V)^2 dV + \alpha/2 \int_{\Omega} \left(q(x,y) \right)^2 d\Omega \qquad (17)$$

In Fig. 9 and 10 the frame highlights the area of observation and corresponding adjustment of the flow Ω_{obs}.

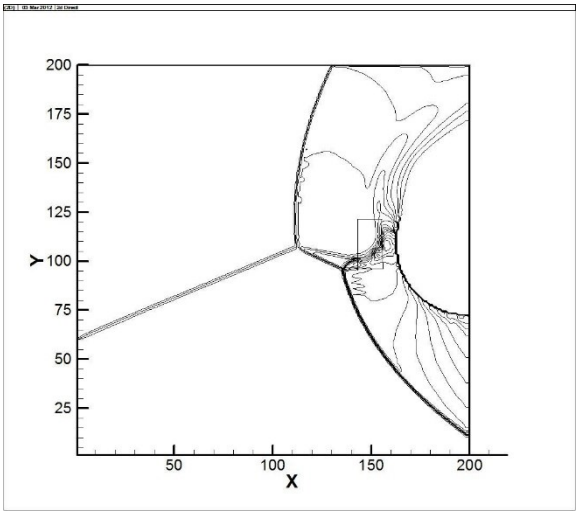

Figure 9. Target current (isolines ρ) *IV* type

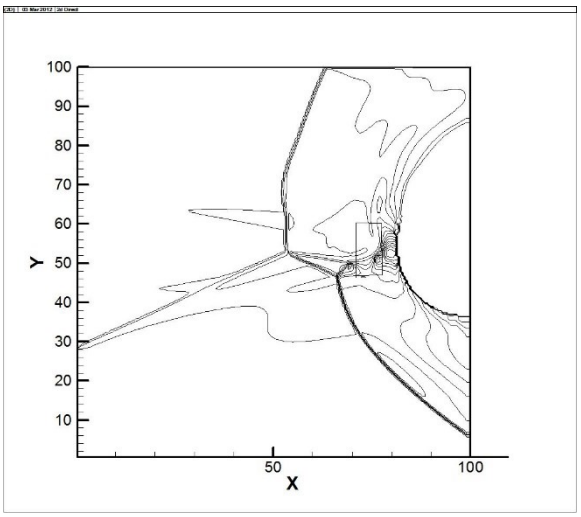

Figure 10. Reproducing the target flow in the window (isolines ρ).

to completely match the fields in Ω_{obs}, but the residual functional decreases by an order of magnitude. Figure 11 shows the location of heat sources. It was possible to reduce the maximum pressure by half while consuming energy $\eta = 0.048$.

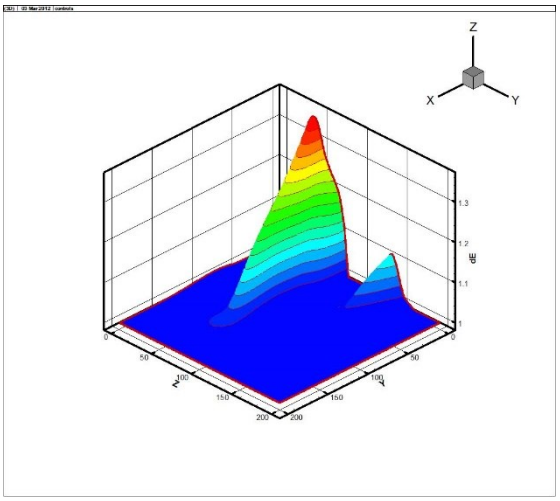

Figure 11. Density of a heat source during a targeted transition to flow type *IVa*

Thus, reproducing a certain “target” flow that has the desired properties is also possible by controlling parameters on the body.

6. Discussion

Generally speaking, it is quite easy to find heat sources capable of destroying a low-entropy jet, which represents the main danger from the point of view of high values of static pressure on the surface. This is due to the relatively narrow range of parameters within which *IV* the genus interaction exists. More difficult is the search for an impact that is minimal in terms of the total power of heat sources.

Three different options for choosing a control action are considered. The first uses a “thermal needle” [1] and completely rebuilds the flow field by forming a front separation zone.

The second is based on the refraction of the shock wave in the heated region and the displacement of the intersection point of the incident and direct shocks, which transforms the interaction from type *IV* to type *V* in accordance with the results of [5].

The third is based on an automatic search for the distribution of heat sources by solving the inverse problem. As part of solving the inverse problem, the minimization of the control action norm is carried out using a regularizing addition to the objective functional. The maximum surface pressure and energy consumption depending on the regularization coefficient are given in Table 1.

Table 1.

α	$P_{\max}$	η
0.001	0.73	0.88
0.01	1.542	0.23
1.0	2.3	0.0247

Regularization makes it possible to reduce the integral power of the heat source below the results [5] (where $\eta = 0.068$) , but at the same time increases the maximum pressure, which is natural when moving from a “thermal needle” type structure containing a separation zone. The search for minimal control by solving the inverse problem is complicated by the search for the optimal regularization coefficient. Purposeful transformation of flow from type IV to type IVa is the simplest from the point of view of the cost of computing resources.

For low powers of heat sources, the change in pressure on the surface is consistent with the sign of the gradient (Fig. 3). For sufficiently powerful sources, close to those used in [5], the destruction of the flow type IV occurs regardless of whether they are placed in the negative or positive region of the gradient. Thus, the nonlinearity of the problem does not allow using the maximum pressure gradient field with respect to heat sources to select control actions . However, when the sources are placed in a region with zero gradient, the flow type IV will remain the same for much more powerful sources.

Conclusion

Considered the following ways to control the flow in the interaction mode IV using distributed heat sources:

- Deflection of an incident shock wave when passing through a heated region with transformation of the interaction of shocks from type IV to type V .
- Formation of a “thermal needle” using a local intense heat source.
- -to-type IVa shock interactions IV using distributed heat sources of moderate intensity.

The calculation results indicate that the transformation of interaction type IV into type IVa requires less energy. It is also possible to purposefully transform a type structure IV into a type IVa if information about the desired flow field is available.

Solving the problem of finding heat sources that reduce the pressure on the surface of the cylinder during the interaction IV of shocks is possible using gradient optimization and solving conjugate equations. Numerical experiments have shown that both the integrals of the pressure functions on the body surface and the discrepancy between the current and target flow parameters in the computational field can be used as target functionals . In this case, the search for the source with the minimum integral value significantly depends on the choice of the regularization coefficient. Visual representation of the flow control process is an integral part of process control.

When solving the problem of controlling the interaction of shocks, it is necessary to simultaneously visualize the flow field, the field of conjugate parameters (sensitivity coefficients) and the field of heat sources $f_i(t,x,y),\psi_i(t,x,y),Q(t,x,y)$, which makes it possible to determine the zones and intensity of the impact and the corresponding results.

References

1. *Georgievsky P.Yu., Levin V.A.,* Supersonic flow around a body in the presence of external heat sources // Letters to the Technical Physics. 1988, T. 14, pp. 684-687.
2. *Knight, D., Kuchinskiy, V., Kuranov, A., and Sheikin, E.* , Survey of Aerodynamic Flow Control at High Speed by Energy Deposition, AIAA Paper 2003-0525.
3. *Adelgren R.G., Yan H., Elliott G.S., Knight D.D., Beutner T.J., and Zheltovodov A.A.* Control of Edney IV Interaction by Pulsed Laser Energy Deposition // AIAA J.-2005.- V. 43, No. 2.-P. 256-263.
4. *Yan H., Gaitonde D.,* Effect of Energy Pulse on 3-D Edney IV Interaction, AIAA J. 2008. V. 46. No. 6. P. 1424-1431.
5. *Kogan M.N., Starodubtsev M.A.,* Reducing peak heat flows by adding heat to the oncoming flow, Fluid Dynamics, N 1, 2003, 134-146
6. *Alekseev A.K.,* Control of the transition between regular and mach reflection of shock waves, Computational Mathematics and Mathematical Physics, 2012, Volume 52, Issue 6, Pages 976–983, DOI: https://doi.org/10.1134/S0965542512060036
7. *Alekseev A.K.,* On the transition between the regular and Mach modes of interaction of shock waves under the influence of temperature perturbations // Fluid Dynamics N 5, 2012, pp. 95-101
8. B. Edney, Effects of Shock Impingement on the Heat Transfer around Blunt Bodies. *AIAA J.*, 6(1) (1968) 15-21.
9. *Borovoy V.Ya.,* Gas flow and heat transfer in zones of interaction of shock waves with the boundary layer.-_M.: Mashinostroenie, 1983.-128 p.
10. *Alekseev AK, Navon I.M.* Estimation of goal functional error arising from iterative solution of Euler equations// Int. J. of Comput. Fluid Dyna. 2008. V. 22. No. 4. P. 221-228.
11. *van Leer B.* Towards the ultimate conservative difference scheme. V. A second-order sequel to Godunov's method//J. Comput. Phys. 1979. V. 32. P. 101–136
12. *Toro EF* Riemann Solvers and Numerical Methods for Fluid Dynamics, Berlin: Springer Verlag. 2006. P. 724
13. *Sun M., Katayama K.* An artificially upstream flux vector splitting for the Euler equations // JCP. 2003. V. 189. P. 305-329.
14. *Yamamoto S., Daiguji H.* Higher-order-accurate upwind schemes for solving the compressible Euler and Navier-Stokes equations// Computers and Fluids . 1993. V. 22. P. 259-270.
15. *Farooq M. A., Muller B. ,* Accuracy assessment of the Cartesian grid method for compressible inviscid flows using a simplified ghost point treatment, J. of Structural Mechanics, V. 44, No. 3, 2011, pp. 279-291.
16. *Gorsse Y., Iollo A., Telib H., Weynans L., A simple second order Cartesian scheme for compressible Euler flows. Inria , RR -7773. 2011. P . 24*
17. *Vinnikov V.V., Reviznikov D.L.,* Cartesian grids methods for numerical solution of Navier–Stokes equations in domains with curvilinear boundaries// Mathematical Modeling, 2005, v. 17, no. 8, p. 15-30.
18. *Toro E. and Siviglia A.* PRICE: Primitive centered schemes for hyperbolic system of equations// Int . Journal for Numerical Methods in Fluids. 2003 V. 42 P. 1263–1291.
19. *Borovoy V. Ya., Chinilov A. Yu ., Gusev VN, Struminskaya IV, Delery J. and Chanetz B.,* Interference Between a Cylindrical Bow Shock and a Plane Oblique Shock//AIAA J. 1197. V. 35, no. 11. P. 1721-1728.
20. *Alekseev A.K., Bondarev A.E.,* Adjoint Method Application and Adjoint Parameters Visualization for Flow Control and Identification and for Validation and Verification Problems, Scientific Visualization, 2011, T. 3, N 3, p . 1-22/